Available online at www.eccomasproceedia.org
Eccomas Proceedia COMPDYN (2021) 4015-4025

ECCOMAS
Proceedia

COMPDYN 2021
8th ECCOMAS Thematic Conference on
Computational Methods in Structural Dynamics and Earthquake Engineering
M. Papadrakakis, M. Fragiadakis (eds.)
Streamed from Athens, Greece, 28 - 30 June 2021

VARIATION IN RESPONSE OF A BRIDGE SEISMICALLY ISOLATED WITH LRBS UNDER THE EFFECT OF LOW AMBIENT TEMPERATURE

E. Cavdar[1], V. Karuk[1], G. Ozdemir[1]

[1]ESQUAKE Seismic Isolator Test Laboratory, Eskisehir Technical University
Eskisehir, Turkey
e-mail: esengulcavdar@eskisehir.edu.tr

{volkankaruk, gokhan_ozdemir}@eskisehir.edu.tr

Abstract

In this paper, the change in response parameters of a seismically isolated bridge, namely maximum isolator displacement (MID) and shear force (MSF), is studied when the ambient temperatures drops to (-30ºC) from 20ºC. Isolation system of the analyzed bridge is assumed to be composed of lead rubber bearings (LRBs). First, the LRB was subjected to cyclic loading after a conditioning period of 24 hours at both temperatures. Test results were used to validate the success of analytical model used to idealize the deteriorating hysteretic behavior of the LRB. Then, verified analytical representation of LRB was utilized in nonlinear response history analyses in order to measure the variation in MID and MSF in the bridge model under the effect of bidirectional seismic excitations at 20ºC and -30ºC. Two distinct group of ground motions, that constitute characteristics of both near-field and large-magnitude-small-distance records, were used in the analyses. Results showed that MIDs obtained for LRB properties of 20ºC are about 20% larger than the ones obtained for -30ºC, in an average sense. Furthermore, average MSF obtained for near-field ground motions at 20ºC and -30ºC are identical. However, for large-magnitude-small-distance ground motions, MSF of -30ºC is almost 25% larger than that of 20ºC.

Keywords: Seismic Isolation, Ambient Temperature, Nonlinear Analysis, Lead Rubber Bearing, Strength Deterioration.

ISSN:2623-3347
Peer-review under responsibility of the organizing committee of COMPDYN 2021.
doi: 10.7712/120121.8764.19139

1 INTRODUCTION

Seismic isolation is an earthquake protection system which is used for new and retrofit construction in many countries such as Japan, Italy, United State and Turkey. Its low horizontal stiffness enables the natural period of the structure lengthening, hence, in case of maximum earthquake shaking isolation systems are reduce the force demands and superstructure remain elastic behavior. Among broad classes of seismic isolation systems, lead rubber bearing (LRB) is the most popular used seismic isolator type. In these units, rubber layers reinforced by steel plates and a lead core placed at the center passes through the height of the bearing. The use of steel plates responsible for reducing the bulge and increasing the vertical stiffness of the bearing whereas lead core supplies the required strength in horizontal direction.

The usage area of LRB has been extensively increase around the world since it was invented, such as bridge, hospital, residential building, data centers. In parallel, several research has been conducted to understand the change in mechanical properties of LRB isolators, namely post yield stiffness and characteristic strength, under the effect of different parameters [1-7]. One of these parameters is the change in ambient temperature in which either affects rigidity of rubber [8-14] or needs to modify of LRB properties at low temperatures [15-17] under the effect of cyclic loading. In particular, Hasegawa et al. [15] tested a LRB which is 250 mm in diameter with a lead core diameter of 38 mm. Displacement controlled LRB tests were conducted at temperatures of 40, 20, 0 and -20°C for a shear strain of 100% at 0.3 Hz. Similarly, Constantinou et al. [4] conducted tests with an LRB having rubber and lead core diameters of 381 mm and 70 mm, respectively. On the other hand, rather than displacement-controlled test results, seismic performance of bridges, isolated by LRBs, under the effects of both ground motion excitations and low temperature have also been investigated. For instance, Billah and Todorov [18] investigated the seismic response of an LRB isolated bridge in case of subfreezing temperature. Authors performed nonlinear response history analyses (NRHA) using a bridge model subjected to different ground motions representative of earthquakes in Eastern Canada. In their study, LRBs were modeled with two different non-deteriorating bilinear force-displacement curves to idealize hysteretic behavior of LRBs at “summer” (25°C) and “winter” (-30°C) with properties provided by manufacturer. Another study that has focused on seismic response of LRB isolated bridge under low temperature was conducted by Deng et al. [19]. Similarly, in the analytical model, they used a non-deteriorating hysteretic representation for LRBs where stiffness and strength of LRB was modified in accordance with an empirical formulation. LRB properties used in the analyses were computed for temperatures changing from -30°C to 40°C. However, it is to be mentioned that both Billah and Todorov [18] and Deng et al. [19] neglected the deterioration in strength of LRBs due to temperature rise in the lead core under cyclic motion. Thus, presented results are based on bounding analyses where hysteretic properties such as strength and stiffness of LRB do not change during the applied motion.

Detailed review of the literature for seismic response of LRB isolated bridges at low temperatures revealed that (i) results regarding the variation in mechanical properties of LRB isolators are based on either small- or moderate-size bearings (ii) analytical models for isolator behavior at low temperature do not address the deteriorating hysteretic behavior of LRBs. Thus, there is a need to revisit the performance of LRB isolated bridges subjected to ground motion excitations at low temperature.

The objective of this study is to determine the variation in seismic performance of an LRB isolated bridge considering the change in mechanical properties of LRB when exposed to low temperature. For this purpose, first, a large-size LRB was tested at both room (20°C) and low

(-30°C) temperatures under dynamic conditions. Change in mechanical properties of tested LRB was reported. Then, experimental data is used to verify the success of analytical model employed to idealize hysteretic response of LRBs. Accordingly, deteriorating hysteretic behaviors of the LRB obtained from both experiments and analytical models were compared with each other. Once the use of analytical model to idealize nonlinear hysteretic behavior of LRBs has been shown to be appropriate for both room and low temperature conditions, a representative bridge seismically isolated by LRBs, was analyzed under the effect of both near-field and large-magnitude small-distance ground motions. In the analyses, both horizontal components of selected ground motions were subjected to structural model simultaneously. Maximum isolator displacements (MIDs), and maximum isolator forces (MIFs) were the response quantities used to quantify the variation in seismic performance of LRB isolated bridge at low temperature.

2 EXPERIMENT OF A LARGE-SIZE LEAD RUBBER BEARING

2.1 Specimen

The bearing tested in this study is a large-size LRB with rubber and lead core diameters of 1020 mm and 190 mm, respectively. Height of the bearing is 436 mm including the top and bottom plates together with the end shim at the top. It is composed of 28 layers of rubber each of which has 10 mm thickness with a total rubber height of 280 mm. Geometrical properties of the tested LRB is presented in Figure 1.

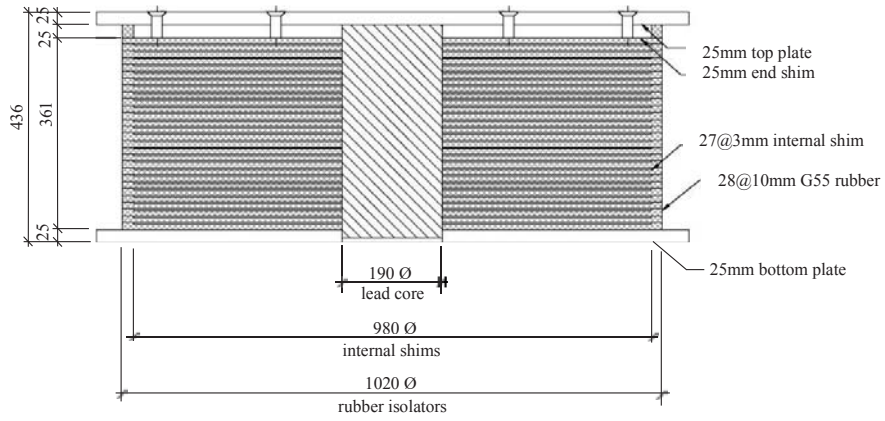

Figure 1- Section cut of test specimen

2.2 Loading Device

Tests were conducted at ESQUAKE Seismic Isolator Test Laboratory of Eskisehir Technical University. Figure 2.a, b shows the air-conditioned room and test setup used in the experiment, respectively. The temperature capacity of the air conditioning room is between -40ºC and + 50ºC. In the loading device, vertical actuator has the maximum capacity of 20000kN load. In the horizontal actuator, the maximum capacity of 2000kN load and ±600 mm stroke with 1000mm/s velocity.

2.3 Loading Method

In order to determine the mechanical properties of the specimen, its hysteretic response in shear was recorded under a constant compressive load. Accordingly, the LRB was subjected to three cycles of sinusoidal motion with amplitude equals to 280 mm that corresponds to

100% shear strain. Frequency of the motion was 0.1 Hz where the maximum velocity is 176 mm/s. The LRB was first tested at a temperature of 20°C after conditioning for 24 hours inside the laboratory and tested again at a temperature of -30°C after conditioning for 24 hours inside the air-conditioned room (Figure 2.a). In all experiments described in this paper, vertical load is equal to 4500kN (6MPa normal stress).

(a) (b)

Figure 2 - (a) Air-conditioned room and (b) seismic isolator test setup of ESQUAKE

2.4 Test Results

Mechanical properties of the tested LRB such as post-yield stiffness (K_d), characteristic strength (Q_d), effective stiffness (K_{eff}), energy dissipation capacity (EDC) and effective damping ratio (ξ_{eff}) are computed by means of Equations (1)-(4) provied by ISO 22762-1 [20]. In Equations (1) and (2), Q_1', Q_1'', Q_2' and Q_2'' are the isolator forces at 50% of the maximum positive and negative horizontal displacements d_{max} and d_{min}. Q_1 and Q_2 of Equation (3) are the isolator forces at d_{max} and d_{min}, respectively (see Figure 3). The calculated test results of LRB isolator are presented in Table 1 for temperatures of 20°C and -30°C.

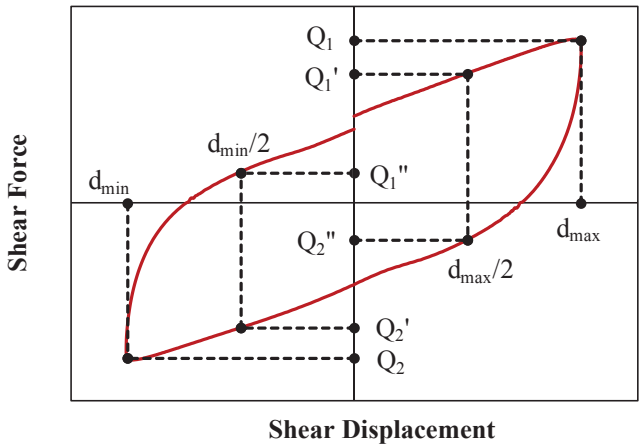

Figure 3 - Force-displacement definitions for LRBs.

$$Q_d = \left[\frac{Q_1'' d_{max}/2 - Q_1' d_{min}/2}{(d_{max} - d_{min})/2} - \frac{Q_2' d_{max}/2 - Q_2'' d_{min}/2}{(d_{max} - d_{min})/2} \right] / 2 \qquad (1)$$

$$K_d = \left[\frac{Q_1' - Q_1''}{(d_{\max} - d_{\min})/2} + \frac{Q_2'' - Q_2'}{(d_{\max} - d_{\min})/2} \right] / 2 \tag{2}$$

$$K_{eff} = \left[\frac{Q_1 - Q_2}{d_{\max} - d_{\min}} \right] \tag{3}$$

$$\xi = \left[\frac{EDC}{\pi(F_{\max} D_{\max} + F_{\min} D_{\min})} \right] \tag{4}$$

Temperature	Cycle	Q_d (kN)	K_d (kN/m)	K_{eff} (kN/m)	EDC (kN·m)	ξ_{eff} (%)
-30°C	1	489	2020	3441	504	0.29
	2	414	1919	3100	433	0.28
	3	372	1864	2913	382	0.26
20°C	1	324	1833	2706	335	0.25
	2	286	1796	2510	297	0.24
	3	260	1766	2392	264	0.22

Table 1: Mechanical properties of LRB at 20°C and -30°C.

According to the test results, it can be revealed that characteristic strength Q_d of the tested LRB increases when the temperature drops down to -30°C. The amount of amplification in Q_d is 50% for the first cycle whereas it is 45% and 43% for the second and third cycles, respectively. Similarly, post-yield stiffness K_d of the LRB increases 10% as the temperature decreases for first cycle. On the other hand, energy dissipation capacity (EDC), increases as the temperature decreases. In parallel, reducing the temperature from 20°C to -30°C contributes to an increase in effective damping ratio ξ_{eff} equal to 17% for the first cycle. Considering the obtained results, it can be noted that variation in mechanical properties of LRB is not constant while different air temperatures expose to the bearing.

3 ANALYTICAL REPRESENTATION OF LRB ISOLATED BRIDGE MODEL

3.1 Hysteretic Response of LRB

The analytical representation of the tested LRB were performed by means of OpenSees [21] structural analysis program. Force-displacement curves obtained from experiments are compared with the analytical ones for both 20°C and -30°C. Figure 4 shows that hysteretic response of the tested LRB can be idealized realistically with great success in the analyses regardless of the ambient temperature. During the LRB model, mathematical representation proposed by Kalpakidis and Constantinou [22] can be considered to modify the initial strength of lead as a function of lead core temperature. Their model considers the instantaneous temperature rise in the lead core and allows calculating the reduction in strength of isolator via reducing the initial yield stress of the lead, instantly. For detailed information please refer to Kalpakidis and Constantinou [22].

3.2 Bridge Model

Analyzed bridge model is a cast-in-place concrete box girder bridge with a 30-degree skew. The length of the bridge is 97.5m and has three spans with lengths of 30.5m, 36.5m and

30.5m. Intermediate bents consist of two 1.22m circular columns and a cap beam with dimensions of 1.22mx1.83m. The total weight of the bridge above the isolation level is 24956 kN (box girder and each diaphragm weigh 229 kN/m and 657 kN, respectively). The section at one of the intermediate bents is presented in Figure 5.a.

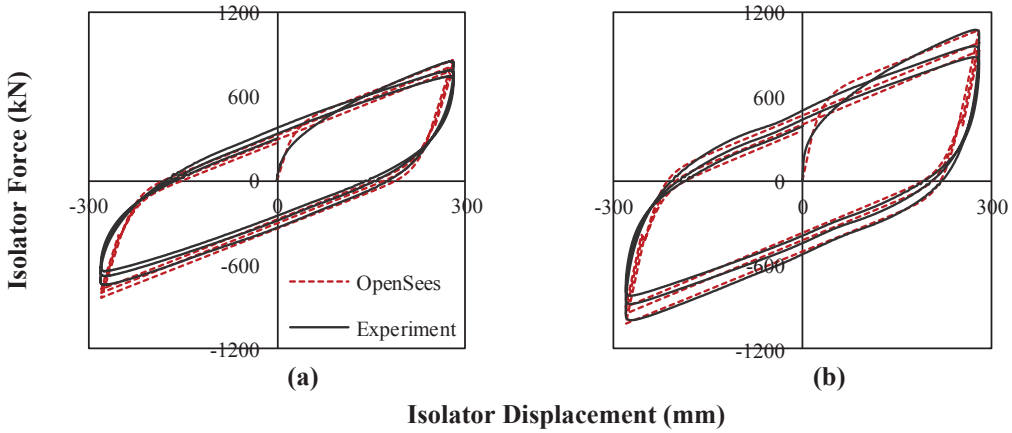

Figure 4: Comparison of experimental and analytical hysteretic curves of LRB tested at a)20°C and b)-30°C.

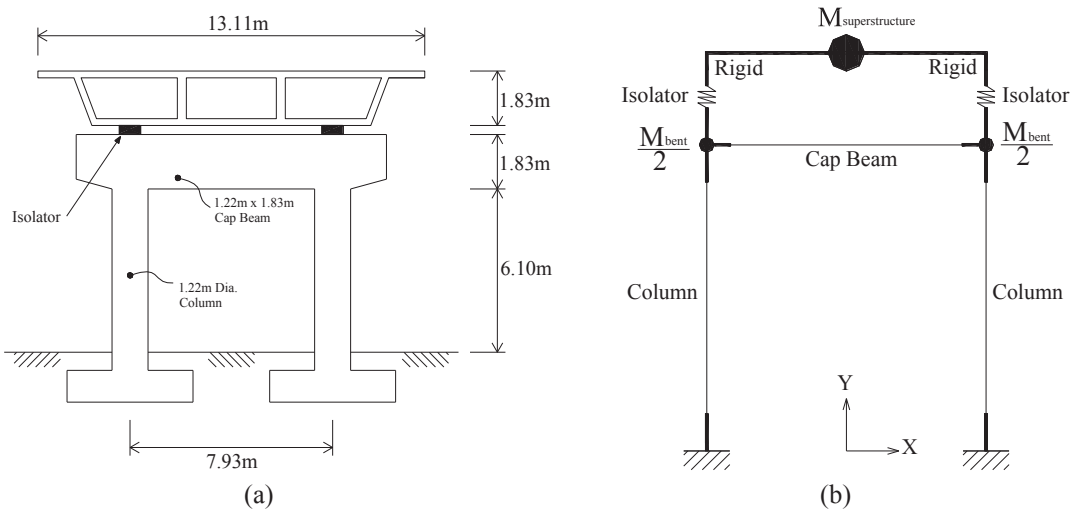

Figure 5: (a) bent geometry and (b) analytical model of the bent.

As shown in Figure 5.a, seismic isolation system is composed of two LRBs at each abutment and pier with a total of eight isolators. They are modeled by deteriorating hysteretic behavior. In order to consider nonlinear bidirectional interaction of LRBs in case of simultaneous excitations of ground motions in both horizontal directions, bidirectional hysteretic model developed by Park et al [23] was employed in the model.

The bridge superstructure was assumed to have infinite in-plane rigidity [24-25]. Analytical representation of the bridge bent is given in Figure 5.b where $M_{superstructure}$ is defined based on the tributary weight of the superstructure + the additional weight of the diaphragm and equals to 850t (isolation period based on the post-yield stiffness of the tested LRB at 20^{o}C is 3s). Total mass of the bent components, M_{bent}, is lumped equally at the column tops. In the analytical model, member rigid end zone matter is also taken into account to represent the bent stiffness properly. The bridge superstructure and columns are modeled as elastic based on the assumption that structure remains within the elastic range due to seismic isolation by means of *elasticbeamcolumn* element of OpenSees [21]. Accordingly, the elastic

modulus of concrete is taken as 24820 MPa. Bridge structure is assumed to be fixed at the foundation level.

4 GROUND MOTIONS

Two sets of ground motions previously used by Warn and Whittaker [24], were considered in the analyses. Each ground motion set is composed of 10 pairs of record. They were clustered to represent characteristics of near-field (NF) and large-magnitude small-distance (LMSD) records. The magnitudes of ground motions grouped as near-field are in between 6.7 and 7.6 with closest distances to the fault rupture less than 10 km. On the other hand, large-magnitude small-distance ground motions have magnitudes greater than 6.5 while closest distances to fault rupture are in between 10 km and 30 km. Tables 2 and 3 give the characteristics of the considered ground motions where PGA, PGV and PGD stands for peak ground acceleration, peak ground velocity and peak ground displacement, respectively.

#	Event	Station	M_w	Comp.	PGA	PGV	PGD	Distance
1	Tabas, Iran	Tabas	7.4	FN FP	0.90 0.98	109.7 105.8	55.5 74.9	1.2
2	Loma, Prieta	Lex Dam	7.0	FN FP	0.69 0.37	178.7 68.7	56.6 25.4	6.3
3	Cape Mendocino	Petrolia	7.1	FN FP	0.64 0.65	62.9 46.5	14.1 10.3	8.5
4	Erzincan, Turkey	Erzincan	6.7	FN FP	0.43 0.46	119.1 58.1	42.1 29.5	2.0
5	Landers	Lucerne	7.3	FN FP	0.71 0.80	136.1 70.3	11.2 184.3	1.1
6	Northridge	Rinaldi	6.7	FN FP	0.89 0.39	174.2 60.9	38.3 17.3	7.5
7	Northridge	Olive View	6.7	FN FP	0.73 0.60	122.1 53.9	30.7 9.1	6.4
8	Kobe	JMA	6.9	FN FP	1.09 0.57	160.2 72.4	40.1 15.9	3.4
9	Chi-Chi, Taiwan	TCU065	7.	West North	0.81 0.60	126.2 78.8	92.6 60.8	1.0
10	Chi-Chi, Taiwan	TCU075	7.6	West North	0.33 0.26	88.3 38.2	86.5 33.2	1.5

Table 2 - Characteristics of selected near-field ground motions.

#	Event	Station	M_w	Comp.	PGA	PGV	PGD	Distance
1	Loma Prieta	Gilroy Array #1	6.9	0 90	0.41 0.47	31.6 33.9	6.4 8.5	11.2
2	Kocaeli, Turkey	Gebze	7.4	0 270	0.24 0.14	50.3 29.7	42.8 27.6	17.0
3	Loma Prieta	Saratoga Aloha Ave	6.9	0 90	0.51 0.32	41.2 42.6	16.3 27.6	13.0
4	Cape Mendocino	Rio Dell Over Pass FF	7.1	270 360	0.39 0.55	43.8 41.9	21.7 19.5	18.5
5	Landers	Joshua Tree	7.3	0 90	0.27 0.28	27.5 43.1	9.5 14.3	11.6
6	Loma Prieta	Gilroy Array #2	6.9	0 90	0.37 0.32	32.9 39.1	7.2 12.1	12.7
7	Landers	Yermo Fire Station	7.3	270 360	0.25 0.15	51.4 29.7	43.9 24.6	24.9
8	Kobe	Abeno	6.9	0 90	0.22 0.24	20.7 24.2	9.1 10.0	23.8
9	Duzce, Turkey	Bolu	7.1	0 90	0.73 0.82	56.4 62.1	23.1 13.6	17.6
10	Northridge	Canoga Park Topanga Can	6.7	106 196	0.36 0.42	32.1 60.7	9.1 20.3	15.8

Table 3: Characteristics of selected large-magnitude small-distance ground motions.

5 DYNAMIC ANAYLSES RESULTS

Nonlinear response history analyses were performed in OpenSees [21] with due consideration of deteriorating hysteretic representation of LRBs under bidirectional excitations of ground motions given Tables 2 and 3 in order to evaluate the variation in response quantities of the SIB due to change in environmental temperature. Accordingly, maximum isolator displacements (MIDs) and base shears in the pier are presented in a comparative manner for 20°C and -30°C.

5.1 Maximum Isolator Displacement

This section presents the observations related to variation of MID of the analyzed structural system due to change in ambient temperature. Figure 6 shows the comparison of MIDs obtained for 20°C and -30°C for both ground motion sets of NF and LMSD. Averages of MIDs recorded for all of the considered ground motion records are also given in Figure 6 where MIDs were calculated by taking the maxima of $\sqrt{(D_x^2 + D_y^2)}$. Here, D_x and D_y are the isolator displacements in horizontal x- and y-directions, respectively. Figure 6.a, at which MIDs for NF ground motions are presented, reveals that MID reduces significantly when the ambient temperature drops down from 20°C to -30°C. The amount of reductions in MID ranges from 8% to 53% with an average value of 19%. Similar comparison for LMSD ground motions is given in Figure 6.b. In this case, the amounts of change in MIDs for individual ground motion records range from 33% to -52% with an average of -16%.

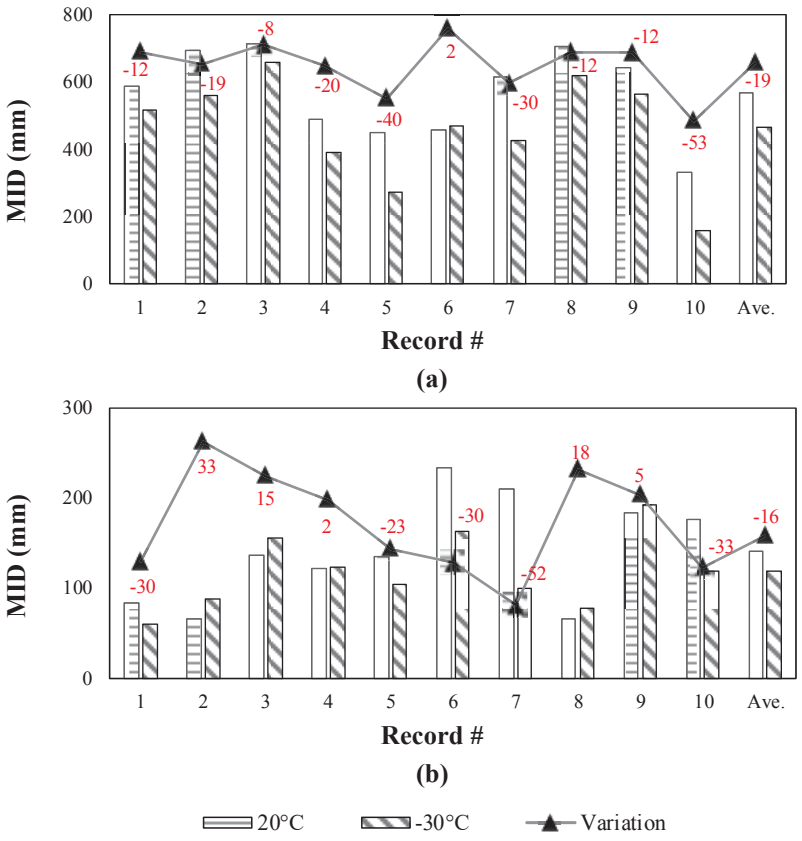

Figure 6: Comparison of MIDs for (a) NF and (b) LMSD ground motions at 20°C and -30°C.

5.2 Maximum Base Shear in the Piers

In this section, variation of base shears acting on each column of the bridge is presented in Figure 7 as a function of ambient temperature and seismicity level. For near field ground motions, Figure 7.a shows that the amounts of variation in isolator force are in between -13% to 20% when temperature decreases from 20°C to -30°C. However, it is interesting to observe that when the averages of base shears are of concern, they are identical for both 20°C to -30°C with a magnitude of 1248 kN. Although the initial strength and stiffness of isolator increases due to reduced ambient temperature, the average shear force does not change for both 20°C to -30°C. Figure 7.b is depicted to investigate the variation of isolator force for large-magnitude small-distance ground motion set when temperature is reduced from 20°C to -30°C. Figure 7.b reveals that although the average value of amplification in isolator force is calculated as 23%, for the selected ground motions it may be up to 60%, individually.

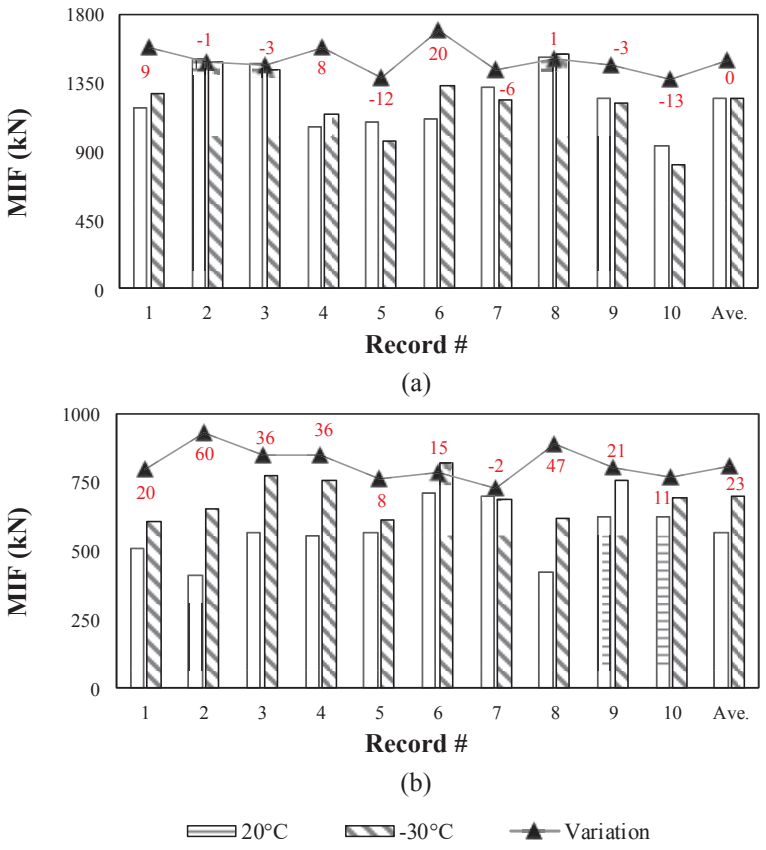

Figure 7: Comparison of MIFs for (a) NF and (b) LMSD ground motions at 20°C and -30°C.

6 CONCLUSIONS

In this paper, variation in response parameters of a seismically isolated bridge is studies under the effect of low (-30°C) and air temperature (20°C). The major findings showed that MIDs obtained for LRB properties of 20°C are about 20% larger than the ones obtained for -30°C, in an average sense. Furthermore, average MSF obtained for near-field ground motions at 20°C and -30°C are identical. However, for large-magnitude-small-distance ground motions, MSF of -30°C is almost 25% larger than that of 20°C.

REFERENCES

[1] W.H. Robinson, Lead Rubber Hysteretic Bearings Suitable for Protecting Structures During Earthquake, *Earthquake Engineering and Structural Dynamics*, 10(4), 593–604, 1982.

[2] S. Nagarajaiah, X. Sun, Response of Base Isolated USC Hospital Building in Northridge Earthquake, *Journal of Structural Engineering (ASCE)*, 126(10), 1177-1186, 2000.

[3] C.W. Roeder, Proposed Design Method for Thermal Bridge Movements, *Journal of Bridge Engineering*, 8(1), 12-19, 2003.

[4] M.C. Constantinou, A.S. Whittaker, Y. Kalpakidis, D.M. Fenz, G.P. Warn, Performance of Seismic Isolation Hardware Under Service and Seismic Loading, *Technical report*, *NY: MCEER=07-2012*, Buffalo, 2007.

[5] G. Benzoni, C. Casarotti, Effects of Vertical Load, Strain Rate and Cycling on The Response of Lead-Rubber Seismic Isolators, *Journal of Earthquake Engineering*, 13(3), 293-312, 2009.

[6] H. Erdoğdu, E. Çavdar, G. Özdemir, Türk Deprem Yönetmelikleri (DBYBHY ve TBDY) Spektrum Tanımlarının Deprem Yalıtım Sistemi Tasarımı Özelinde Karşılaştırılması, *Teknik Dergi*, 32(5), 2021.

[7] S. Pinarbasi, U. Akyuz, Sismik İzolasyon ve Elastomerik Yastik Deneyleri. *İMO Teknik Dergi*, 237, 3581-3598, 2005.

[8] C.W. Roeder, J.F. Stanto, A.W. Taylor, *Performance of Elastomeric Bearings* (No. 298). Washington, DC: National Cooperative Highway Research Program, Transportation Research Board, 1987.

[9] D.F. Ritchie, *Neoprene Bridge Bearing Pads, Gaskets and Seals*. Rubber World, Lippincott & Petto Inc. 200(2), 27–31, 1989.

[10] R. Eyre, A. Stevenson, Performance of Elastomeric Bridge Bearings at Low Temperatures, *Proceedings 3rd World Congress on Joint Sealing and Bearing Systems for Concrete Structures*, 736-762. Toronto, Canada, 1991.

[11] A. Yakut, J.A. Yura, Evaluation of Low-Temperature Test Methods for Elastomeric Bridge Bearings, *Journal of Bridge Engineering*, 7(1), 50-56, 2002(a).

[12] A. Yakut, J.A. Yura, Parameters Influencing Performance of Elastomeric Bearings at Low Temperatures, *Journal of Structural Engineering*, 128(8), 986–994., 2002(b).

[13] K.N.G. Fuller, J. Gough, A.G. Thomas, The Effect of Low-Temperature Crystallization on The Mechanical Behavior of Rubber, *Journal of Polymer Science: Part B: Polymer Physics*, 42(11), 2181-2190, 2004.

[14] D. Cardone, G. Gesualdi, D. Nigro, Effects of Air Temperature on The Cyclic Behavior of Elastomeric Seismic Isolators, *Bulletin of Earthquake Engineering*, 9(4), 1227–55, 2011.

[15] O. Hasegawa, I. Shimoda, M. Ikenaga, Characteristic of Lead Rubber Bearing by Temperature. *Summaries of Technical Papers of Annual Meeting Architectural Institute of Japan*, B-2, Structures II, Structural Dynamics Nuclear Power Plants, Architectural Institute of Japan, pp: 511-512, 1997.

[16] C.B. Cho, I.J. Kwahk, Y.J. Kim, An Experimental Study for The Shear Property and The Temperature Dependency of Seismic Isolation Bearings, *Journal of the Earthquake Engineering Society of Korea*, 12(1), 67-77, 2008.

[17] J.Y. Park, K.S. Jang, H.P. Lee, Y.H. Lee, H. Kim, Experimental Study on The Temperature Dependency of Full-Scale Low Hardness Lead Rubber Bearing, *Journal of Computational Structural Engineering*, 25(6), 533-540, 2012.

[18] M. Billah, B. Todorov, Effects of Subfreezing Temperature on The Seismic Response of Lead Rubber Bearing Isolated Bridge, *Soil Dynamics and Earthquake Engineering*, 126, 1-13, 2019.

[19] P. Deng, Z. Gan, T. Hayashikawa, T. Matsumoto, Seismic Response of Highway Viaducts Equipped with Lead-Rubber Bearings Under Low Temperature, *Engineering Structures*, 209:110008, 2019.

[20] ISO (International Organization for Standardization). ISO 22762-1:2005: Elastomeric seismic-protection isolators – Part 1: Test methods, 2005.

[21] OpenSees, Open System for Earthquake Engineering Simulation; Version: 2.1.0, University of California, Pacific Earthquake Engineering Research Center, Berkeley, California, 2001.

[22] I.V. Kalpakidis, M.C. Constantinou, Effects of Heating on The Behavior of Lead-Rubber Bearings. I: Theory, *Journal of Structural Engineering*, 135(12), 1440–1449, 2009a.

[23] Y.J. Park, Y.K. Wen, A.H. Ang, Random Vibration of Hysteretic Systems Under Bi-Directional Ground Motions, *Earthquake Engineering and Structural Dynamics*, 14(4), 543-557, 1986.

[24] G.P. Warn, A.S. Whittaker, Performance Estimates in Seismically Isolated Bridge Structures, *Engineering Structures*, 26(9), 1261–78, 2004.

[25] M. Dicleli, Performance of Seismic-Isolated Bridges in Relation to Near-Fault Ground-Motion and Isolator Characteristics, *Earthquake Spectra*, 22(4), 887-907, 2006.